

Analysis of Turnouts with Non-linear Curvature of Diverging Track for Different Train Running Speeds

Władysław KOC¹

Summary

The paper deals with the issue of shaping variable curvature in diverging track of a railway turnout. A solution without a circular arc in the central zone, containing two zones of non-linear curvature with the same length and zero curvature values at the end points, was adopted as a model, on the basis of previously conducted dynamic tests. The optimum type of curvature was selected from the perspective of the kinematic conditions. An analytical record of the curvature and the tangent inclination angle along the diverging track and of the Cartesian coordinates of the diverging track are presented. The obtained theoretical correlations were verified by computing. Verified correlations were used to determine geometrical parameters of some turnouts with non-linear curvature of the diverging track for different assumed train running speeds on it. The criterion was to minimize the length of the entire turnout with a predefined ordinate of the end of its diverging track.

Keywords: railway turnouts, diverging track, curvature modelling

1. Introduction

Railway turnout matters have been discussed in many publications [1–5, 7, 15, 18, 20–21], especially in those dealing with high speed railways [6, 17, 22–23]. Turnout construction itself is permanently changing, however, in an ordinary turnout, the typical geometrical shape of the diverging track is a single circular arc without transition curves. Such a solution is not used on track sections without turnouts and this results in the necessity to restrict train running speeds. Speed restrictions arise from the presence of locations with abrupt leap changes of the ordinates on the curvature graph at the beginning and end of the turnout. Recently in some countries, especially in high speed railways, attempts to soften the curvatures in such locations have taken place. This is achieved by introducing so-called “clothoid sections”, on both ends of the circular arc, on which curvature changes linearly, frequently however without reaching zero values at extreme points [17, 19, 22–23], as shown in Figure 1. Theoretical analysis for such a case has been conducted in one paper [9]. An alternative solution applying sections with non-linear curvature is proposed in another study [12] (see Fig. 2).

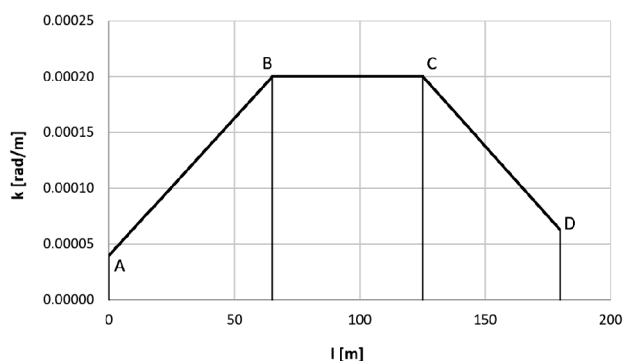


Fig. 1. Example graph representing diverging track curvature of a turnout with linear sections ($R_1 = 16\,000$ m, $l_1 = 55$ m, $R_2 = 6000$ m, $l_2 = 60$ m, $l_3 = 65$ m, $R_3 = 25\,000$ m) [own elaboration]

The length of the turnout diverging track is split into three zones:

- l_1 length of the start zone with curvature changing from the k_1 value (at point A) to the k_2 value (point B),
- l_2 length of the middle zone with a constant curvature value k_2 (between points B and C),
- l_3 length of the end zone with curvature changing from the k_2 value (point C) to the k_3 value (point D).

¹ Prof. Ph.D., M.Sc., Eng.; Gdańsk University of Technology; Department of Rail Transportation and Bridges; e-mail: kocwl@pg.edu.pl.

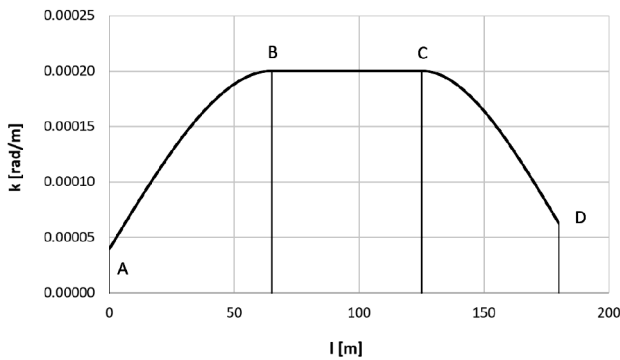


Fig. 2. Example graph representing diverging track curvature of a turnout with non-linear sections ($R_1 = 16\ 000\ m$, $l_1 = 55\ m$, $R_2 = 6000\ m$, $l_2 = 60\ m$, $l_3 = 65\ m$, $R_3 = 25\ 000\ m$) [own elaboration]

Kinematic parameters determine the circular arc radius value (in other words, curvature k_2) as well as the lengths of sections with variable curvature for a predefined train running speed. Of course, different variants of solutions are possible, linked with curvature values and the lengths of individual zones. This also allows free determination of the turnout slope and its end ordinate [11].

2. Searching for the optimum solution

At this point, a key question should be asked – which set of turnout characteristic values, i.e. k_1 , k_2 and k_3 as well as l_1 , l_2 and l_3 , is optimal in a certain situation? The list of possible variants is significantly restricted by dynamic analysis, which has been shown in some studies [13, 14]. A dozen or so application cases, comprising sections with linear and non-linear curvature, are considered. For non-linear curvature, a condition was set to keep a permitted value of the increase in acceleration as well as an increase of this value by 50%. Figures 3 and 4 show example graphs of oscillation movements for turnout diverging track sections with linear curvature, with non-zero and zero curvature values at the start and end points.

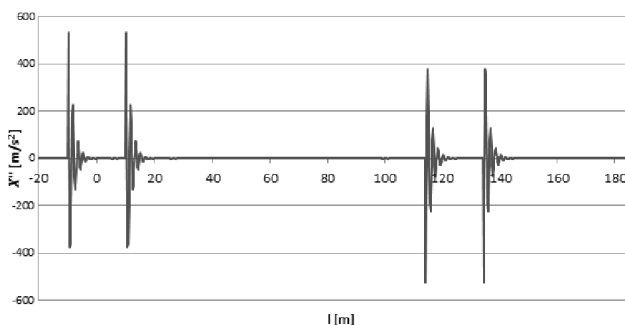


Fig. 3. Graphs of acceleration of oscillation movements for linear curvature sections and the values $k_1 = k_3 = 1/8000\ rad/m$ [14]

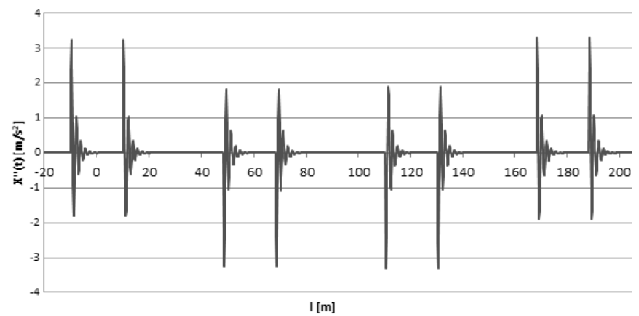


Fig. 4. Graphs of acceleration of oscillation movements for linear curvature sections and the values $k_1 = k_3 = 0$ [14]

As can be seen, setting zero curvature values at the start and end points ensures incomparably lower values of dynamic impact. This finding has been fully proven for cases applying non-linear sections, for which the obtained values are significantly lower. The optimum solution, i.e. the one which is characterised by lower values of dynamic impact (accelerations), is the case with non-linear curvature sections of the same length, zero curvature at the start and end of the turnout, which respects the binding value of the permissible increase of acceleration. Figure 5 shows a graph representing curvature along diverging track for this exact case.

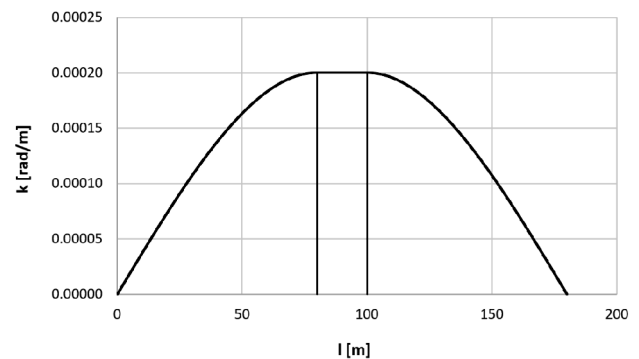


Fig. 5. Optimum graph of curvature along diverging track of a turnout with non-linear sections ($k_1 = 0$, $l_1 = 86\ m$, $k_2 = 1/6000\ rad/m$, $l_2 = 12.484\ m$, $l_3 = 86\ m$, $k_3 = 0$) [own elaboration]

In comparison with the model graphs shown in Figures 1 and 2, the level of steering values went down by half. Here it is possible to change the subdivision of the length of the turnout diverging track into zones:

- l_1 length of the start zone with curvature changing non-linearly from zero to the value $k = 1/R$,
- l_2 length of the middle zone with a constant curvature value $k = 1/R$,
- $l_3 = l_1$ length of the end zone with curvature changing non-linearly from the value $k = 1/R$ to zero.

The ideal curvature distribution shown in Figure 5 formed the subject of detailed analysis conducted in one work [10]. It has demonstrated that:

- enlarging the radius R results in the ability to minimize the lengths of the sections with non-linear curvature, in consequence leading to shortening of the whole turnout and minimizing its end ordinate and slope $1 : n$ (namely an increase in the n value),
- introducing a relatively short middle zone, with set high R values, can be seen as an optimal solution; its application gives a shorter overall length of the turnout (of course, that may not be deemed important, disregarding the required diverging track end ordinate),
- obtaining an assumed end ordinate when introducing the middle zone (i.e. section of a circular arc) in each case causes elongation of the entire turnout in comparison with variants without this zone; that is why such a solution does not seem sensible.
- the ability to change the turnout slope by achieving the value n as an integer appears to be a more complex issue due to the presence of a lower number of variable parameters, which may be manipulated; in most cases this starts to be possible only after elimination of the middle zone and assuming a slightly larger end ordinate.

The case without a circular arc zone (i.e. $l_2 = 0$), on the basis of the above statements, has been accepted as an optimum solution. At the same time, it was necessary to introduce the symbol $l_1 = l_3 = l_k$.

3. Analytical solution of the problem

Curvature modelling on the length of the turnout diverging track allows its analytical notation to be created in the form of the function $k(l)$, where the l parameter defines the location of a certain point on the length of the curve. Coordinate equations for the sought connection can be written down in a parametrical form [8]:

$$x(l) = \int \cos \Theta(l) dl \tag{1}$$

$$y(l) = \int \sin \Theta(l) dl \tag{2}$$

The tangent inclination angle function $\Theta(l)$ is defined by the formula

$$\Theta(l) = \int k(l) dl \tag{3}$$

3.1. Problem solution for the start zone

Applying sections with non-linear curvature means that in a start zone (for $l \in \langle 0, l_k \rangle$) the following border conditions take effect:

$$\begin{cases} k(0) = 0 & k(l_k) = k \\ k'(0) = C \frac{k}{l_k} & k'(l_k) = 0 \end{cases} \tag{4}$$

while the differential equation is

$$k^{(4)}(l) = 0, \tag{5}$$

where the numerical coefficient $C \geq 0$.

Following the parametrical equation is obtained as a result of solving the differential problem (4), (5):

$$k(l) = k \left(\frac{C}{l_k} l - \frac{2C-3}{l_k^2} l^2 + \frac{C-2}{l_k^3} l^3 \right) \tag{6}$$

while the tangent inclination angle function $\Theta(l)$ is described by the relationship

$$\Theta(l) = k \left(\frac{C}{2l_k} l^2 - \frac{2C-3}{3l_k^2} l^3 + \frac{C-2}{4l_k^3} l^4 \right) \tag{7}$$

$$\text{At the end of the start zone } \Theta(l_k) = \frac{6+C}{12} k l_k.$$

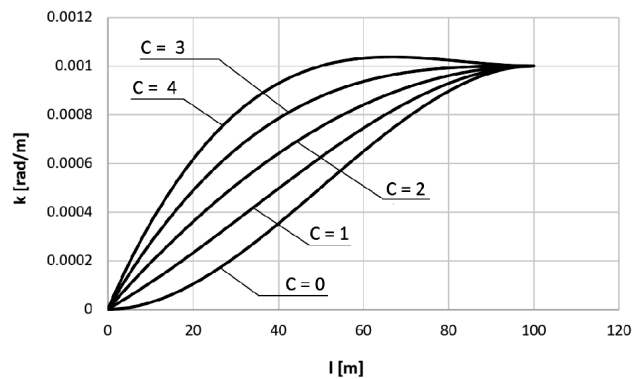


Fig. 6. Example curvature graphs on the length of the new transition curve for chosen coefficient C values ($R = 1000$ m, $l_k = 100$ m) [own elaboration]

Figure 6 shows an example of the curvature graphs in the length domain for chosen values of the C coefficient. As can be seen, monotonic flow of the curvature is characterised by curves for $C \in \langle 0; 3 \rangle$. The curve for $C = 0$ has the softest flow, however – similarly as for other curves – fulfilment of the requirement to respect permissible increase of acceleration requires its elongation in comparison to a reference curve with linear curvature.

However, when choosing the optimum curve from the analysed curves, one should first apply the crite-

tion of the minimum required length. This length is determined – aside from train running speed – by the permissible increase of acceleration, which is directly linked with the derivative of the curvature.

$$k'(l) = \frac{C}{Rl_k} - \frac{2(2C-3)}{Rl_k^2}l + \frac{3(C-2)}{Rl_k^3}l^2 \quad (8)$$

Figure 7 shows graphs of the derivative of the curvature on the length of the transition curve, for which $C \in \langle 0; 2,5 \rangle$.

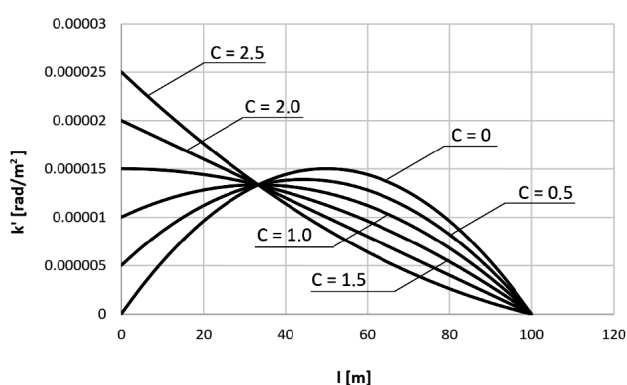


Fig. 7. Example graphs of the derivative of the curvature on the length of the new transition curve for chosen values of the C coefficient ($R = 1000$ m, $l_k = 100$ m) [own elaboration]

As the derivative $k'(l)$ described by equation (8) changes in length domain, its maximum value counts. For the coefficient $C \in \langle 0; 1,5 \rangle$, the maximum value of $k'(l) = k'(l_0)$, where the location of the l_0 point, in which the maximum of the function $k'(l)$ appears, is derived from the condition

$$k''(l) = -\frac{2(2C-3)}{Rl_k^2} + \frac{6(C-2)}{Rl_k^3}l_0 = 0$$

which results in

$$l_0 = \frac{2C-3}{3(C-2)}l_k \quad (9)$$

The l_0 value determined by equation (9) substituted in equation (8) determines the maximum of the $k'(l)$ function.

$$\max k'(l) = \left[C - \frac{(2C-3)^2}{3(C-2)} \right] \frac{1}{Rl_k} \quad (10)$$

For $C > 1,5$, the l_0 value determined by equation (10) does not fulfil requirements of the task (obtained $l_0 > l_k$ or alternatively obtained l_0 relates to the func-

tion minimum). However, $\max k'(l) = k'(0)$ as $k'(l)$ reaches its maximum value at the start point.

The necessary elongation grade of the sought transition curve in comparison with the basic clothoid, associated with the necessity to preserve permissible increase of acceleration, determines the ratio of the $\max k'(l)$ to the derivative $k'(l)_{lin}$ appearing on the linear curvature, which is a constant value described by the formula:

$$k'(l)_{lin} = \frac{1}{Rl_k} \quad (11)$$

For $C = 0$, the value of the $\max k'(l) / k'(l)_{lin} = 3/2$. Therefore, due to permissible increase of acceleration, length of the transition curve has to be longer by 50% than for the linear curvature. On the other hand, for $C = 1$, the value of the $\max k'(l) / k'(l)_{lin} = 4/3$, which means that the length of this curve has to be longer than the clothoid only by 1/3. Consequently, performed analysis shows that the optimum solution is the one with the coefficient $C = 1$. This leads to following equations for the functions $k(l)$ and $\Theta(l)$:

$$k(l) = k \left(\frac{1}{l_k}l + \frac{1}{l_k^2}l^2 - \frac{1}{l_k^3}l^3 \right) \quad (12)$$

$$\Theta(l) = k \left(\frac{1}{2l_k}l^2 + \frac{1}{3l_k^2}l^3 - \frac{1}{4l_k^3}l^4 \right) \quad (13)$$

The function $\Theta(l)$ enables the determination of parametrical equations $x(l)$ and $y(l)$ for this zone by using relationships (1) and (2). The Maxima program [16] was used for expanding the functions $\cos \Theta(l)$ and $\sin \Theta(l)$ into Maclaurin series. Then, individual words were integrated.

$$x(l) = l - \frac{k^2}{40l_k^2}l^5 - \frac{k^2}{36l_k^3}l^6 + \frac{5k^2}{504l_k^4}l^7 + \frac{k^2}{96l_k^5}l^8 + \left(\frac{k^4}{3456l_k^4} - \frac{3k^2}{864l_k^6} \right) l^9 \quad (14)$$

$$y(l) = \frac{k}{6l_k}l^3 + \frac{k}{12l_k^2}l^4 - \frac{k}{20l_k^3}l^5 - \frac{k^3}{336l_k^3}l^7 - \frac{k^3}{192l_k^4}l^8 + \frac{k^3}{2592l_k^5}l^9 \quad (15)$$

At the end of the zone, the tangent inclination angle is:

$$\Theta(l_k) = \frac{7}{12}kl_k.$$

3.2. Problem solution for the end zone

In the end zone (for $l \in \langle l_k; 2l_k \rangle$) the following border conditions take effect:

$$\begin{cases} k(l_k) = k & k(2l_k) = 0 \\ k'(l_k) = 0 & k'(2l_k) = -C \frac{k}{l_k} \end{cases} \quad (16)$$

and the differential equation (5). The obtained result of the differential problem (5), (16) is the following:

$$k(l) = k \left(2C - 4 + \frac{12 - 5C}{l_k} l - \frac{9 - 4C}{l_k^2} l^2 + \frac{2 - C}{l_k^3} l^3 \right) \quad (17)$$

The tangent inclination angle equation has the following form

$$\Theta(l) = k \left[\frac{2 - C}{2} l_k + (2C - 4)l + \frac{12 - 5C}{2l_k} l^2 - \frac{9 - 4C}{3l_k^2} l^3 + \frac{2 - C}{4l_k^3} l^4 \right] \quad (18)$$

At the end of the zone, the value of the angle $\Theta(l)$ equals:

$$\Theta(2l_k) = \frac{6 + C}{6} k l_k.$$

For the agreed coefficient $C = 1$, the equations $k(l)$ and $\Theta(l)$ are as follows:

$$k(l) = k \left(-2 + \frac{7}{l_k} l - \frac{5}{l_k^2} l^2 + \frac{1}{l_k^3} l^3 \right) \quad (19)$$

$$\Theta(l) = k \left(\frac{1}{2} l_k - 2l + \frac{7}{2l_k} l^2 - \frac{5}{3l_k^2} l^3 + \frac{1}{4l_k^3} l^4 \right) \quad (20)$$

At the end of the curve, the tangent inclination angles:

$$\Theta(2l_k) = \frac{7}{6} k l_k.$$

Parametrical equations were received after expanding the functions $\cos \Theta(l)$ and $\sin \Theta(l)$ into Taylor series using the Maxima program [16] and integrating individual words:

$$\begin{aligned} x(l) = & x(l_k) + \cos \Theta(l_k)(l - l_k) - \frac{k}{2} \sin \Theta(l_k)(l - l_k)^2 - \\ & + \frac{k^2}{6} \cos \Theta(l_k)(l - l_k)^3 + \frac{k^3}{24} \sin \Theta(l_k)(l - l_k)^4 + \\ & + \frac{k^4}{120} \cos \Theta(l_k)(l - l_k)^5 \end{aligned} \quad (21)$$

$$\begin{aligned} y(l) = & y(l_k) + \sin \Theta(l_k)(l - l_k) + \frac{k}{2} \cos \Theta(l_k)(l - l_k)^2 - \\ & + \frac{k^2}{6} \sin \Theta(l_k)(l - l_k)^3 + \\ & - \frac{k^3}{24} \cos \Theta(l_k)(l - l_k)^4 + \frac{k^4}{120} \sin \Theta(l_k)(l - l_k)^5 \end{aligned} \quad (22)$$

Basic turnout dependency applies:

$$\tan \Theta(2l_k) = \frac{1}{n} \quad (23)$$

4. Scope of conducted analysis

The theoretical dependencies presented above are subject to calculation verification – they are used to derive geometrical parameters for a few turnouts with variable curvature of the diverging track for the assumed train running speeds $V_{div} = 40, 80$ and 120 km/h on this track. If a commonly assumed assumption is taken that the train speed on the turnout diverging track equals half of the train speed on the track section without turnouts (in other words, on the main track), then the last given value applies to high speed railways. It is assumed that such turnouts are foreseen for connecting parallel tracks with a distance between track centres equal to 4 m (without a straight insert), giving the end ordinate of their diverging track equal to 2 m.

Minimum values of the parameters occurring on the railway turnout diverging track are determined for the assumed train running speed: radius of the circular arc R in the middle of the arrangement as well as the lengths l_k of the sections with variable curvature. They are limited by permissible values of respective kinematic parameters.

The minimum radius of the circular arc in the middle part is calculated using the formula

$$R_{min} = \left(\frac{V}{3.6} \right)^2 \frac{1}{a_{dop}} \quad (24)$$

where a_{per} means the permissible value of the uncompensated acceleration.

Taking into account equations (12) shows that on the length of sections with non-linear curvature (for the coefficient $C = 1$) lateral acceleration $a(l)$ exists, as described by the equation

$$a(l) = \left(\frac{V}{3.6} \right)^2 k \left(\frac{1}{l_k} l + \frac{1}{l_k^2} l^2 + \frac{1}{l_k^3} l^3 \right) \quad (25)$$

The value of the increase $\psi = \frac{V}{3.6} \frac{d}{dl} a(l)$ of acceleration changes in the length domain and, therefore, the following condition is in force:

$$\psi_{\max} = \max \left[\left(\frac{V}{3.6} \right)^3 k \left(\frac{1}{l_k} + \frac{2}{l_k^2} l + \frac{3}{l_k^3} l^2 \right) \right] \leq \psi_{dop}.$$

where ψ_{per} means permissible increase of acceleration.

From the analysis conducted in point 3.1, it appears that, in the case of the investigated curve, the value ψ_{\max} occurs at the point $l_0 = l_k / 3$; and, therefore, finally should be:

$$\psi_{\max} = \frac{4}{3} \left(\frac{V}{3.6} \right)^3 \frac{k}{l_k} \leq \psi_{dop}.$$

The formula for the minimum length of the sections with non-linear curvature is therefore the following:

$$\min l_k = \frac{4}{3} \left(\frac{V}{3.6} \right)^3 \frac{k}{\psi_{dop}} \quad (26)$$

After determining the coordinates of the end of the diverging track $x(2l_k)$ and $y(2l_k)$, as well as the tangent inclination angle $\Theta(2l_k)$, it becomes possible to determine the location of the middle of the turnout as well as the length of its through track. The turnout middle point lies on the axis of the through track at the distance:

$$x_O = x(2l_k) - \frac{y(2l_k)}{\tan \Theta(2l_k)} \quad (27)$$

from the beginning of the turnout, on the other hand, the length of the through track is

$$l_{zas} = x_O + \frac{y(2l_k)}{\sin \Theta(2l_k)} \quad (28)$$

5. Establishing geometrical parameters

Table 1 contains a consolidated sheet with geometrical parameters of the turnout diverging track for chosen train running speeds during an iterative approach to the end ordinate 2 m. The parameter l_{div} represents the length of the turnout diverging track ($l_{\text{div}} = 2 l_k$).

Table 1

Sheet with generated variants' characteristic values for chosen train running speeds during an iterative approach to the end ordinate 2 m

V_{div} [km/h]	R [m]	l_k [m]	l_{div} [m]	l_{thr} [m]	$\Theta(l_{\text{div}})$ [rad]	n	$x(l_{\text{div}})$ [m]	$y(l_{\text{div}})$ [m]
40	350	18	36	36.004	0.06000	6.64666	35.968	1.187
	290	21	42	42.009	0.08448	11.80856	41.927	1.949
	290	21.27	42.54	42.550	0.08557	11.65794	42.464	1.9998
	290	21.28	42.56	42.570	0.08561	11.65244	42.484	2.0017
	290	21.271	42.542	42.552	0.08578	11.65739	42.466	2.00002
	290	21.272	42.544	42.554	0.08558	11.65684	42.468	2.00021
80	600	82	164	164.129	0.15944	6.21854	162.985	14.327
	1200	41	82	82.004	0.03986	25.07382	81.968	1.797
	1200	43.25	86.50	86.505	0.04207	23.76798	86.463	1.9999
	1200	43.26	86.52	86.525	0.04206	23.76248	86.483	2.0009
	1200	43.251	86.502	86.507	0.04205	23.76743	86.465	2.00002
	1200	43.252	86.504	86.507	0.04208	23.76688	86.467	2.00011
120	1500	110	220	220.050	0.08556	11.65978	219.607	10.341
	2600	64	128	128.003	0.02872	34.81186	127.974	2.021
	2700	61	122	122.003	0.02636	37.93032	121.979	1.768
	2650	63	126	126.003	0.02774	36.04518	125.976	1.922
	2650	64.26	128.52	128.523	0.02829	35.33804	128.495	1.9995
	2650	64.27	128.54	128.543	0.02830	35.33254	128.515	2.0001
	2650	64.267	128.534	128.537	0.02829	35.33419	128.509	1.99994
	2650	64.268	128.536	128.539	0.02829	35.33364	128.511	2.00002
	2650	64.269	128.538	128.541	0.02829	35.33309	128.513	2.00006

[Own elaboration].



5.1. Turnout for the speed of $V_{\text{div}} = 40$ km/h

The value $R_{\text{min}} = 145.243$ m is obtained for the assumed train running speed $V_{\text{div}} = 40$ km/h, assuming a permissible increase of uncompensated acceleration with the value $a_{\text{per}} = 0.85$ m/s², and applying formula (24). In the following performed calculations, the radius of the circular arc $R = 350$ m is assumed to be the initial one, as this R_{min} is a very small value, which creates problems for track negotiation by rolling stock.

The condition stating that $\min l_k = 17.419$ m is received by assuming the permissible increase of acceleration $\psi_{\text{per}} = 0.3$ m/s³ (as for individual transition curves with linear curvature) and applying formula (26). In the performed calculations, the lengths of the sections with non-linear curvature $l_k = 18$ m are assumed to be initial ones.

For the assumed $R = 350$ m and $l_k = 18$ m, a turnout is received with the length of 36.004 m, slope 1:16.64666 and the end ordinate of the diverging track equal to 1.187 m. Thus, the end ordinate diverges from the required value of 2 m. The radius $R = 290$ m and associated length $l_k = 21$ m are achieved by applying an iterative approach, and give the end ordinate equal to 1.949 m. Then, further correction (in other words, enlarging) of the l_k value takes place, keeping the radius $R = 290$ m, and finally results in the required end ordinate. Finally, the accepted geometrical arrangement of the turnout diverging track has the radius $R = 290$ m and the length of the sections with variable curvature $l_k = 21.271$ m. Turnout slope equals 1:11.65739, and the length of the through track equals 42.542 m.

5.2. Turnout for the speed of $V_{\text{div}} = 80$ km/h

The value $R_{\text{min}} = 580.973$ m is obtained for the assumed train running speed $V_{\text{div}} = 80$ km/h, by applying formula (24). Thus, the circular arc radius $R = 600$ m is assumed to be the initial one for the following performed calculations. The condition that the $\min l_k = 81.288$ m is obtained on the basis of formula (26); the lengths of the sections with non-linear curvature $l_k = 82$ m are assumed to be initial ones.

For the assumed initial values $R = 600$ m and $l_k = 82$ m, a turnout is received with the length of 164.129 m, slope 1:6.21854 and the end ordinate of the diverging track equal to 14.327 m. Thus, the end ordinate diverges from the required value of 2 m. It turns out that the basic way to minimize it is to enlarge the radius R . This circumstance is very beneficial and, at the same time, gives the possibility to minimise the lengths of the sections with variable curvature in accordance with condition (26). The radius $R = 1200$ m and the associated length $l_k = 41$ m are achieved by applying an iterative approach, and give the end ordi-

nate equal to 1.797 m. Then, in order to enlarge this ordinate, further correction (in other words, enlarging) of the l_k value takes place, keeping the radius $R = 1200$ m, which results in the required end ordinate. Finally, the accepted geometrical arrangement of the turnout diverging track has the radius $R = 1200$ m and the length of the sections with variable curvature $l_k = 43.251$ m. Turnout slope equals 1:23.76743, and the length of the through track equals 86.507 m.

5.3. Turnout for the speed of $V_{\text{div}} = 120$ km/h

The value $R_{\text{min}} = 1307.19$ m is obtained for the train running speed $V_{\text{div}} = 120$ km/h, by applying formula (24). Thus, the circular arc radius $R = 1500$ m is assumed to be the initial one for the following calculations. The condition that the $\min l_k = 109.739$ m is obtained simultaneously on the basis of formula (26). The lengths of the sections with the non-linear curvature $l_k = 110$ m are assumed to be initial ones.

For the assumed initial values $R = 1500$ m and $l_k = 110$ m, a turnout is received with the length of 220.05 m, slope 1:11.65978 and the end ordinate of the diverging track equal to 10.341 m. Because the end ordinate diverges from the required value of 2 m, it has to be lowered by enlarging the radius R . This leads to shortening of the lengths of the sections with variable curvature in accordance with condition (26). The radius $R \in \langle 2600; 2700 \rangle$ m and associated length $l_k \in \langle 61; 64 \rangle$ m are achieved by applying an iterative approach, for which the end ordinate is $y(l_{\text{zwr}}) \in \langle 1,768; 2,021 \rangle$ m. The radius $R = 2650$ m is assumed in order to achieve the required end ordinate. The respective value $l_k = 63$ m, and respective end ordinate is 1.922 m. The required end ordinate is achieved by correcting (in other words, enlarging) the l_k value. Finally, the accepted geometrical arrangement of the turnout diverging track has the radius $R = 2650$ m and the length of the sections with variable curvature $l_k = 64.268$ m. Turnout slope equals 1:35.33364, and the length of the through track equals 128.539 m.

5.4. Sheet with determined solutions

Table 2 contains characteristic values which were determined for turnouts with the end ordinate 2 m and dedicated for the speeds $V_{\text{div}} = 40, 80$ and 120 km/h.

Figure 8 shows a set of curvature graphs on the lengths of the diverging tracks of individual turnouts. Figure 9 shows graphs of horizontal ordinates. Due to non-comparative scaling in Figure 9, tangents leading from the end of diverging tracks cross those tracks on their lengths, which of course does not take place in reality.

Table 2

Characteristic values determined for turnouts dedicated for the speeds $V_{div} = 40, 80$ and 120 km/h with the end ordinate 2 m

V_{div} [km/h]	R [m]	l_{div} [m]	l_{thr} [m]	$\Theta(l_{div})$ [rad]	n	$x(l_{div})$ [m]	$y(l_{div})$ [m]
40	290	42.542	42.552	0.08578	11.65739	42.466	2.000
80	1200	86.502	86.507	0.04205	23.76743	86.465	2.000
120	2650	128.536	128.539	0.02829	35.33364	128.511	2.000

[Own elaboration].

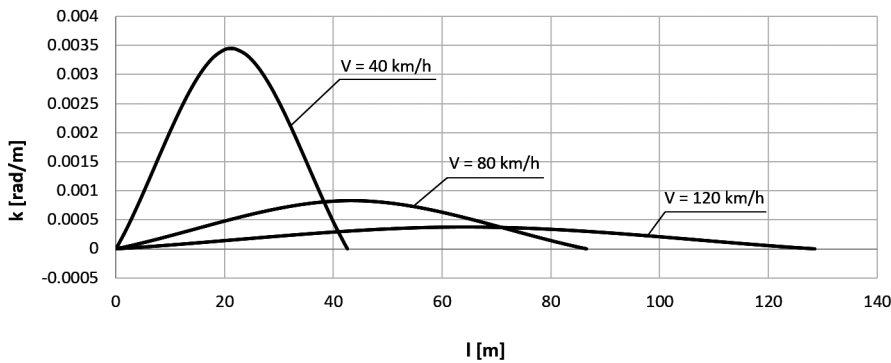


Fig. 8. Curvature graphs on the lengths of the diverging tracks of analysed turnouts [own elaboration]

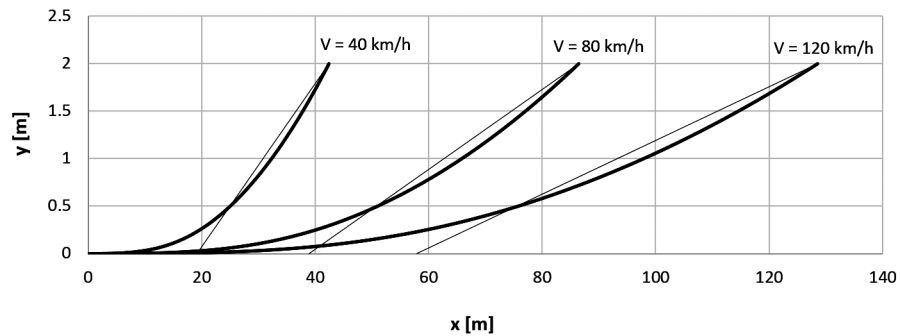


Fig. 9. Graphs of the horizontal ordinates of diverging tracks of analysed turnouts [own elaboration]

6. Practical verification attempt

The presented turnout diverging track shaping concept is an entirely new solution, which up to now has not been applied anywhere in practice. This concept is therefore a proposal, which should be promoted in order to enable its verification in the future. Elimination of regions with abrupt changes in curvature at the beginning and end of the turnout diverging track is a basic advantage of the solution. It arises unambiguously from assumptions adopted for the determination of the curvature equations. However, as the described turnout does not exist yet, it is not possible to assess its operational reliability from the construction point of view [3]. It is only possible to undertake an attempt to analyse switch blade positions in the rail vehicle wheels striking start zone.

Figure 10 shows the outline of a curved switch blade and closure rail position in an example turnout with diverging track variable curvature and in a conventional turnout with diverging track in the form of a circular arc. Both turnouts enable passing with the speed

$V_{div} = 40$ km/h. Geometrical parameters of the first one are given in Table 2 (for the radius $R = 290$ m). The second one is a conventional turnout Rz 300-1:9.

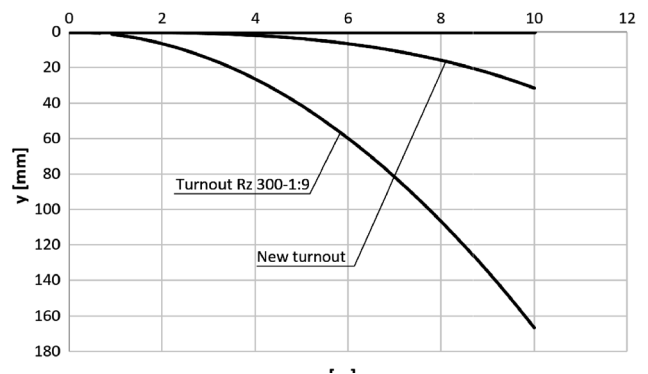


Fig. 10. Outline of the curved switch blade and closure rail position in an example turnout with softened curvature of the diverging track and a traditional turnout (in a non-comparative scale) [own elaboration]

As can be seen, the difference between turnouts is obvious and consistent with expectations. The turn-

out with softened curvature of the diverging track has an elongated switch blade and closure rail adherence zone and gently growing horizontal ordinates. This should translate into better track negotiation by rolling stock wheels, ensuring lower dynamic impact, even running and slower rails wear process in diverging track. These statements arise from logical presumptions and should stack up in real circumstances. Practical verification of the advantages should be based on observing rails wear in diverging tracks of such shaped turnouts.

7. Conclusions

Diverging track of a typical railway turnout (of the ordinary points) is a single circular arc without transition curves. As a result, there are places with abrupt leap changes of the ordinates on the curvature graph at the beginning and end of the turnout. Recently in some countries, attempts to soften the curvature graph in such locations have taken place. So-called “clothoid sections” are introduced on both ends of the circular arc, on which curvature changes in a linear way.

It was demonstrated in some papers [11, 12], as a result of dynamic analysis, that optimum properties are possessed by turnout diverging track with non-linear flow of the curvature in the start zone and end zone and zero curvature values at extreme points of the geometrical arrangement. At the same time, doubts have arisen as to whether applying so-called “clothoid sections” with non-zero curvature values at the start and end points of the diverging track, which takes place in construction practice, is reasonable.

This work shows a problem-solving analytical method with a general and complete character. A solution without a circular arc in the central zone, comprising two zones of non-linear curvature with the same length and zero curvature values at extreme points, was adopted as a model. The optimum type of curvature was selected from the point of view of the kinematic conditions. An analytical record of the curvature and of the tangent inclination angle along the diverging track and of the Cartesian coordinates of the diverging track are presented.

The obtained theoretical dependencies are subjected to calculation verification. They were used to determine geometrical parameters for a few turnouts with variable curvature of the diverging track for the assumed train running speeds $V_{div} = 40, 80$ and 120 km/h on it. Those turnouts are foreseen for connecting parallel tracks with the distance between track centres equal to 4 m (without a straight insert). The criterion was to minimize the length of the entire turnout with a predefined ordinate of the end of its diverging track.

Literature

1. Alfi S., Bruni S.: *Mathematical modelling of train-turnout interaction*, Vehicle System Dynamics, no. 5/2009, Taylor & Francis, pp. 551–574.
2. Bałuch H.: *Optymalizacja układu geometrycznego rozjazdów przeznaczonych do dużego natężenia przewozów i dużych szybkości pociągów*, Problemy Kolejnictwa, tom 12, nr 44/1968.
3. Bałuch H., Bałuch M.: *Eksplatacyjne metody zwiększenia trwałości rozjazdów kolejowych*, Centrum Naukowo-Techniczne Kolejnictwa, Warszawa 2009.
4. Bałuch M.: *Oddziaływania pojazdów szynowych w poszczególnych strefach rozjazdów*, Zeszyty Naukowo-Techniczne SITK RP w Krakowie, z. 124/2005.
5. Bugarin M.R., García Díaz-de-Villegas J.M.: *Improvements in railway switches*, Proceedings of the Institution of Mechanical Engineers, Part F: Rail and Rapid Transit, no. 4/2002, SAGE Publishing, pp. 275–286.
6. Bugarin M., Orro A., Novales M.: *Geometry of high speed turnouts*, Transportation Research Record: Journal of the Transportation Research Board, no. 2261/2011, National Research Council (U.S.), pp. 64–72.
7. Esveld C.: *Modern railway track*, second ed., MRT-Productions, Zaltbommel 2001.
8. Koc W.: *Analytical method of modelling the geometric system of communication route*, Mathematical Problems in Engineering, vol. 2014, Hindawi, Article ID 679817.
9. Koc W.: *Kształtowanie toru zwrotnego rozjazdu z odcinkami krzywizny liniowej*, Problemy Kolejnictwa, z. 174/2017, Warszawa, s. 39–46.
10. Koc W.: *Optimum shape of turnout diverging track with segments of variable curvature*, Journal of Transportation Engineering, Part A: Systems, vol. 145, no. 1/2019, ASCE, 04018077.
11. Koc W.: *Shaping of the turnout diverging track with variable curvature sections*, International Journal of Rail Transportation, no. 4/2017, Taylor & Francis, pp. 229–249.
12. Koc W.: *Zastosowanie odcinków nieliniowej krzywizny w torze zwrotnym rozjazdu kolejowego*, Przegląd Komunikacyjny, nr 7/2017, SITK RP, s. 27–31.
13. Koc W., Palikowska K.: *Dynamic analysis of the turnout diverging track for HSR with variable curvature sections*, World Journal of Engineering and Technology, vol. 5/2017, Scientific Research, pp. 42–57.
14. Koc W., Palikowska K.: *Wyznaczenie optymalnej krzywizny toru zwrotnego w rozjazdach dla kolei dużych prędkości na podstawie analizy dynamicznej*, Przegląd Komunikacyjny, nr 10/2017, SITK RP, s. 2–7.
15. Lichtberger B.: *Track Compendium. Formation, Permanent Way, Maintenance, Economics*, Eurailpress Tetzlaff-Hestra GmbH & Co., Hamburg 2005.



16. Maxima, a Computer Algebra System [online], dostępny na <http://maksima.sourceforge.net> [dostęp: 28 marca 2018].
17. Ping W.: *Design of high-speed railway turnouts. Theory and Applications*. Elsevier Science & Technology, Oxford 2015.
18. Ping W., Xueyi L.: *Computing theories and design methods of CWR turnout*, Southwest Jiaotong University Press, Chengdu 2007.
19. Plank B.: *Linie dużych prędkości realizowane przez VAE*, Prezentacja firmy Voestalpine GmbH, 2007.
20. Prasad A.: *Turnout design: higher diverging speed in the same footprint*, Proceedings of the AREMA 2011 Annual Conference, September 18–21, 2011, Minneapolis, USA.
21. Sadeghi J., Masnabadi A., Mazraeh A.: *Correlations among railway track geometry, safety and speeds*, Proceedings of the Institution of Civil Engineers – Transport, no. 4/2016, ICE Publishing, pp. 219–229.
22. Technical Memorandum: Alignment design standards for high-speed train operation, Prepared by Parsons Brinckerhoff for the California High-Speed Rail Authority, USA, 2009.
23. Weizhu F.: *Major technical characteristics of high-speed turnout in France*, Journal of Railway Engineering Society, no. 9/2009, China Association for Science and Technology, pp. 18–35.